JOURNAL OF CATALYSIS 94, 408–421 (1985)

Acidic Properties of Molybdena–Alumina for Different Extents of Reduction: Infrared and Gravimetric Studies of Adsorbed Pyridine

WILSON SUAREZ,[1] J. A. DUMESIC,[2] AND CHARLES G. HILL, JR.

Department of Chemical Engineering, University of Wisconsin, Madison, Wisconsin 53706

Received October 29, 1984; revised February 26, 1985

Infrared spectroscopy and thermogravimetric studies of adsorbed pyridine, combined with volumetric reduction/oxidation measurements, were used to investigate the acidic properties of molybdena–alumina samples reduced to different extents in hydrogen at 670 K. Pyridine was adsorbed at 420 K and studied after evacuation at progressively higher temperatures ranging from 370 to 670 K. The average molybdenum oxidation state was varied from +6 to +4.7, as monitored by measuring the consumption of hydrogen and the formation of water during reduction and the consumption of oxygen during reoxidation. Infrared spectra of adsorbed pyridine showed the presence of Brønsted acid sites and two types of Lewis acid sites on oxidized molybdena–alumina. The number of Brønsted acid sites increased at low extents of reduction (e.g., an average Mo oxidation state of +5.6) and decreased to zero with further reduction. The Lewis acidity also passed through a maximum with extent of reduction but was not eliminated with reduction. These results are explained by the accepted model for molybdena–alumina in which the surface of alumina is populated with small molybdena clusters. It is proposed that the electronegativity of alumina is altered in the vicinity of these molybdena clusters, thereby altering the acidic properties.

INTRODUCTION

Molybdena–alumina catalysts have been investigated extensively in an effort to understand the nature of their catalytically active sites. These catalysts have been studied in oxidized, reduced, and sulfided forms with the purpose of determining how changes in catalyst structure are related to observed catalytic properties. In addition, the effects of the preparation variables on the final properties of the catalyst have been the subject of several investigations. The literature on molybdenum-based hydrodesulfurization catalysts has been reviewed by Schuit and Gates (*1*), Massoth (*2*), and Grange (*3*). The present study focuses on the changes in the acidic properties of molybdena–alumina upon reduction in hydrogen.

As Jeziorowski and Knözinger (*4*) have indicated, many studies have been carried out to determine the effects of the preparation variables on the final properties of molybdena–alumina catalysts. Wang and Hall (*5*) have reported that tetrahedral, monomeric Mo species may exist at low molybdenum loadings (e.g., 3 wt%). At higher loadings (e.g., 8 wt%) polymeric species exist. At still higher loadings (>12 wt% Mo) a MoO_3 phase is formed. An $Al_2(MoO_4)_3$ phase can also be formed if the catalyst is calcined at high temperatures (>1000 K) (*2*). Cheng and Schrader (*6*) and Jeziorowski and Knözinger (*4*) found that the state of aggregation of the molybdenum on alumina is independent of the state of the molybdenum species present in the solutions used for incipient wetness impregnation. It has, therefore, been argued that when the incipient wetness method is used, the pH of the small volume of solution present in the pores of the catalyst is changed by the large buffer capacity of the alumina surface.

Wang and Hall (*7*) developed a method of impregnation in which the support is placed

[1] Permanent address: W. R. Grace Co., Research Division, 7379 Route 32, Columbia, Md. 21044.

[2] To whom correspondence should be addressed.

0021-9517/85 $3.00

in contact with a large volume of a very dilute (e.g., <0.05 *M*) solution of ammonium molybdate for a long period of time (~100 h). In this way the pH of the solution in the pores of the support is not changed appreciably by the support. Most of the impregnation achieved using this method is obtained by adsorption, not by precipitation from the solution in the pores. The pH of the solution determines the species in solution and the resultant loading. This is the method of sample preparation which was used in the present study.

Massoth (*8*) used gravimetric methods to study the reduction of molybdena–alumina catalysts. He found that on reduction an appreciable amount of hydrogen was retained by the catalyst and suggested that this hydrogen was present as hydroxyl groups associated with molybdenum. Later, Hall and co-workers (*9, 10*) designed reduction/oxidation experiments using a volumetric system to measure the extent of reduction and the amount of hydrogen retained by the catalyst. They found that two types of adsorbed hydrogen were produced during reduction: reversibly adsorbed hydrogen that could be removed by evacuation at the reduction temperature, and irreversibly adsorbed hydrogen. They measured the quantity of each type of hydrogen, as well as the number of anion vacancies produced, as a function of the extent of reduction. They associated anion vacancies with Mo^{+4} species and the irreversibly adsorbed hydrogen with Mo^{+5} species. In a later paper (*11*) they studied the hydroxyl stretching region of the infrared spectra of reduced catalysts and concluded that the hydroxyl groups introduced by reduction were associated with aluminum atoms and not with molybdenum atoms. The aforementioned volumetric reduction/oxidation methods are employed in the present study to alter systematically the surface properties of molybdena–alumina.

Parry (*12*) was the first investigator to propose the use of the infrared spectroscopy of adsorbed pyridine to characterize the acidity of solid catalysts. Kiviat and Petrakis (*13*) applied this method to the molybdena–alumina system. They showed that addition of molybdenum to the alumina surface produced Brønsted acidity. Two types of Lewis acid sites were found to be present on alumina and molybdena–alumina catalysts. Mone and Moscow (*14*) observed Brønsted acidity for hydrated and calcined molybdena–alumina. Mone (*15*) found Brønsted acidity on an oxidized molybdena–alumina catalyst. Segawa and Hall (*16*) found that the Brønsted acidity could be eliminated by reduction of the catalyst. They also observed that the Brønsted acidity of the oxidized catalyst increased with loading and the Lewis acidity decreased with loading, suggesting that the Lewis acid sites are associated with the alumina surface while the Brønsted acidity depends on the presence of molybdate species. For the reduced catalyst, the Lewis acidity remained constant with molybdenum loading; and it was concluded that Lewis acid sites were present on both the molybdena and alumina portions of the surface. Segawa and Hall (*17*) also studied the chemisorption of nitric oxide and carbon dioxide on molybdena–alumina catalysts; by combining the chemisorption of these two compounds with the chemisorption of pyridine, they concluded that pyridine chemisorbs on both the molybdena and alumina portions of the surface. In the present investigation pyridine was again utilized as a probe molecule in infrared spectroscopy and gravimetric studies of the acidity of molybdena–alumina as a function of reduction treatments.

EXPERIMENTAL

Sample preparation. The sample used in this study was prepared according to the method of Wang and Hall (*7*). A 0.014 *M* solution of $(NH_4)_6Mo_7O_{24} \cdot 4H_2O$ (Matheson, Coleman and Bell AX1310 Reagent) in distilled water was prepared and its pH was adjusted to 4, using HNO_3 and NH_4OH. Twenty grams of η-alumina (Davison High-Surface-Area Alumina Spheres, SMR-7-

5691) were ground to ~80 mesh, calcined for 3 h at 770 K, cooled to room temperature, and placed into the ammonium heptamolybdate solution to effect the impregnation. The mixture was stirred at room temperature for 100 h. The sample was then filtered, dried overnight in air at 380 K, and calcined in air at 770 K for 3 h. The molybdenum loading of the sample was 7.49 wt% and the BET surface area was 211 m^2/g. An alumina blank was prepared by the same procedure except that distilled water was used as the impregnation medium. The BET surface area of this sample was 227 m^2/g.

Reduction–oxidation treatments. The sample was subjected to reduction–oxidation treatments in a volumetric system to alter systematically its surface characteristics, as described by Hall and co-workers (*9, 10*). A detailed description of the apparatus is presented elsewhere (*18*). In short, the main components of this system are the sample cell, an all-glass recirculation pump, a cold trap, a dosing volume, a Texas Instruments precision pressure gauge, and a vacuum system capable of a dynamic vacuum of 10^{-6} Torr.

In a typical experiment 1 g of sample was placed in the sample cell, calcined overnight at 770 K in flowing oxygen, and evacuated at 770 K for 1 h. The sample temperature was then lowered to 670 K for the sequence of steps described below.

A measured amount of hydrogen was admitted into the system and recirculated through the sample bed and subsequently through a trap at 77 K for a specified period of time. The final hydrogen pressure was then determined, and the hydrogen was pumped out of the system through the cold trap for a period of 1 h. The sample was next isolated from the system. The cold trap was warmed to room temperature and the water vapor allowed to expand into the system over a period of 1 h. From a measurement of the final water pressure (typically less than 10 Torr), the amount of water formed during reduction of the catalyst could be determined volumetrically. Following the above reduction measurements, a measured amount of oxygen was introduced in the system and recirculated through the sample bed for 1 h. The final pressure was measured. The experimental conditions used in these reduction/oxidation experiments are summarized in Table 1.

Thermogravimetric and infrared spectroscopy studies were carried out following sample treatments similar to those described above. The sample was calcined overnight at 770 K in flowing oxygen and then evacuated for 1 h at the same temperature. Reduction treatments were subsequently carried out at 670 K using mixtures of helium and hydrogen at atmospheric pressure. The individual flow rates of the two gases were adjusted to give hydrogen partial pressures similar to the final hydrogen pressures obtained in the volumetric reduction–oxidation treatments (see Table 1). The reduction times were also chosen to correspond to those given in Table 1.

The sample was subsequently evacuated for 1.5 h at 670 K, cooled to 420 K, and exposed to pyridine vapor at ca. 4 Torr for 1 h. The sample was then cooled under vacuum (~10^{-3} Torr) to 370 K and further evacuated at this temperature for 1 h. Thermogravimetric or infrared measurements were subsequently made. The sample temperature was then raised under vacuum to 470 K for 1 h, after which thermogravimetric or infrared measurements were again carried out. The same procedure was repeated for final temperatures of 570 and 670 K. The infrared measurements were made at 300 K; the thermogravimetric measure-

TABLE 1

Conditions for Reduction/Oxidation Measurements

Temperature (K)	Time (min)	Initial H_2 pressure (Torr)	Final H_2 pressure (Torr)	Initial O_2 pressure (Torr)
670	5	184	158	187
670	60	187	145	187
670	360	280	230	282

ments were at the temperature of evacuation.

Infrared spectroscopy. Infrared spectra were recorded using a Nicolet 7199 Fourier Transform infrared spectrometer operated with a spectral resolution of 2 cm^{-1}. The samples were examined in the form of self-supporting wafers, prepared by pressing ~75 mg of sample in a 1-in-diameter die to a pressure of 10,000 psi. The infrared spectroscopy cell used in this study has been described elsewhere (*18*). The sample pellet is positioned in a stainless-steel holder supported by two stainless-steel rods. For sample treatment at elevated temperatures, the cell is positioned so that the sample holder is surrounded by a quartz housing which can be heated to 800 K. To record an infrared spectrum at room temperature, the cell is rotated so as to cause the sample holder to move down the steel guide rods to an aluminum section where the sample is positioned between two infrared-transparent windows (CaF_2). This cell can be evacuated to 10^{-5} Torr.

Raman spectroscopy. The Raman spectrometer was a Spex Ramalog 5 (Model 14018) equipped with a third monochromator. The light source was a Spectra-Physics Model 164-06 argon ion laser powered by a Spectra-Physics Model 265 exciter. Rated power output of the laser was 2 W (all lines). The Raman spectrometer was interfaced to a PDP 11/03 minicomputer system to facilitate data acquisition and manipulation. All spectra were recorded using the 488.0-nm line of the argon laser for excitation. The spectra were smoothed and corrected for background fluorescence using procedures described elsewhere (*19*).

To minimize local heating effects where the laser beam impinges on the catalyst sample, a rotating lens assembly was employed. This assembly contains a condenser lens which can be rotated at approximately 1000 rpm. The center of the lens, through which the laser beam passes, is displaced from the axis of rotation. Hence as the lens rotates, the focused laser beam moves in a circle over the surface of the sample. Further details of the apparatus are treated elsewhere (*20*).

Thermogravimetric measurements. Thermogravimetric experiments were carried out using a quartz spring balance manufactured by Ruska Instruments Company. It consists of a quartz spring surrounded by a water jacket, a cathetometer, and a quartz sample compartment which can be heated to 800 K. The changes in sample weight are measured in terms of the displacement of the spring (1 mg corresponding to 1-mm displacement). The sample can be treated in flowing gases or evacuated to a pressure of 10^{-6} Torr. The molybdena–alumina sample and an alumina blank were studied in the form of pellets, prepared by pressing about 400 mg of the appropriate powder in a 1-cm-diameter die to a pressure of 2000 psi. Further details of the above equipment are available elsewhere (*18*).

Purification of gases. Oxygen (99.6%) was purified by passage through an activated molecular sieve column (13X) cooled to 195 K. Helium (99.995%) was passed through a bed of reduced copper turnings maintained at 540 K and then through a 13X molecular sieve column maintained at 78 K. Hydrogen (99.9%) was purified using a Deoxo purifier (Engelhard) followed by a molecular sieve column (13X) held at 78 K.

Pyridine [Aldrich, 99+% purity, Spectrophotometric Grade (Cat. No. 18, 452-7)] was passed over activated 13X molecular sieves. Before use it was degassed using the freeze–pump–thaw technique.

RESULTS

Raman Spectra of Molybena–Alumina

Figure 1 is a Raman spectrum of the oxidized sample after subtraction of the background fluorescence. It shows strong peaks at 951 and 215 cm^{-1} and broader and weaker peaks near 844, 590, and 360 cm^{-1}. The band at 951 cm^{-1} can be assigned to the normal vibrations of Mo=O terminal groups (*4*) of a polyanion or of a monomeric

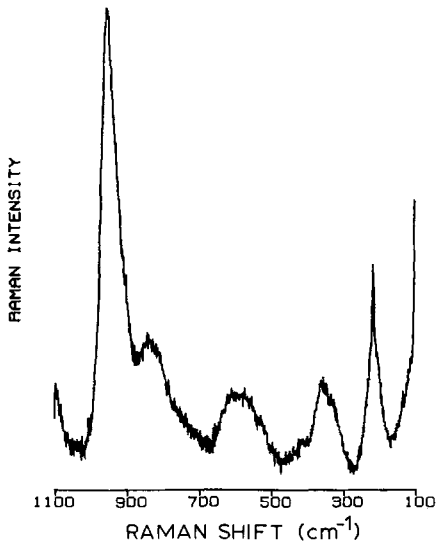

FIG. 1. Baseline-corrected Raman spectrum of oxidized molybdena–alumina.

tetrahedral molybdenum species (*5*). The bands at 844, 590, and 215 cm^{-1} can be assigned to antisymmetric stretching, symmetric stretching, and deformation bands, respectively, due to Mo—O—Mo bonds (*4*). The band at 215 cm^{-1} is strong evidence that Mo—O—Mo bonds are present. Finally, the band at 360 cm^{-1} is produced by Mo=O bending vibrations (*4*). This spectrum is similar to those obtained by Wang and Hall (*5, 21*) for catalysts prepared using the same procedure. It shows that the molybdenum may be present in small polymolybdate clusters.

Reduction/Oxidation Treatments

In general, three quantities are determined from the volumetric reduction/oxidation measurements for the molybdena–alumina sample:

$[H_2]$ ≡ the amount of H_2 which is removed from the gas phase during reduction of the sample

$[W_R^G]$ ≡ the amount of H_2O which is generated during reduction of the sample

$[O_2]$ ≡ the amount of O_2 which is consumed during reoxidation of the sample.

According to Cirillo *et al.* (*22*), the following information can be extracted from these measurements:

$[H_2^I] = 2[O_2] - [W_R^G]$ ≡ amount of H_2 irreversibly adsorbed on the sample after reduction

$[H_2^R] = [H_2] - 2[O_2]$ ≡ amount of H_2 reversibly adsorbed on the sample after reduction

$[H_2^C] = [H_2] - [H_2^R]$ ≡ amount of H_2 consumed that effects reduction of the sample

$[\square] = W_R^G$ = number of oxygen vacancies created during reduction of the sample

$[e] = 4[O_2]$ = total number of electrons added to molybdenum species during reduction of the sample.

The results of such reduction/oxidation measurements for the molybdena–alumina sample of the present study are summarized in Table 2. All quantities are expressed per Mo atom in the sample (i.e., H_C/Mo, H_I/Mo, and H_R/Mo are, respectively, the *atoms* of hydrogen consumed, irreversibly adsorbed, and reversibly held per Mo atom). Some of these results are plotted in Fig. 2 according to the format of Hall and Lo Jacono (*10*). In agreement with the results of these previous investigations, the amount of irreversibly adsorbed hydrogen (H_I/Mo) increases initially with reduction and reaches a maximum of ca. 0.5 when H_C/Mo ≅ 0.8. The number of anion vacancies increases slowly with reduction. However, the number of vacancies per molybdenum atom does not approach the value of 0.5 as H_C/Mo approaches 1.5, a result that was observed by Hall and Lo Jacono (*10*).

Thermogravimetric Analyses

The molybdena–alumina and the alumina samples were calcined and reduced to dif-

TABLE 2

Reduction–Oxidation Results

Time (min)	Temperature (K)	Initial H_2 pressure (Torr)	H_C/Mo	H_I/Mo	□/Mo	H_R/Mo	*e*/Mo
5	670	185	0.39	0.25	0.07	0.12	0.39
5	670	183	0.35	0.18	0.08	0.08	0.35
5	670	184	0.41	0.34	0.04	0.00	0.41
60	670	183	0.68	0.43	0.13	0.16	0.68
60	670	185	0.67	0.52	0.07	0.10	0.67
360	670	286	1.25	0.46	0.14	0.32	1.25
360	670	287	1.23	0.49	0.13	0.20	1.23

ferent extents using the treatments listed in Table 1. The samples were then exposed to pyridine and the extent of adsorption was determined gravimetrically following evacuations at increasingly higher temperatures. The resulting extents of pyridine adsorption (molecules adsorbed per square meter of surface) are listed in Table 3. The total number of pyridine molecules adsorbed is plotted in Fig. 3 against the extent of reduction of the molybdena–alumina sample [H_C/Mo (see Table 2)] for different desorption temperatures. It can be seen that the total number of acid sites (i.e., pyridine adsorption sites) increases during the initial stages of reduction, passes through a maximum, and then decreases at higher extents of reduction. The maximum occurs near H_C/Mo = 0.37. The behavior of alumina following various lengths of treatment in hydrogen at 670 K is quite different. The total number of acid sites decreases initially and then remains constant with reduction time.

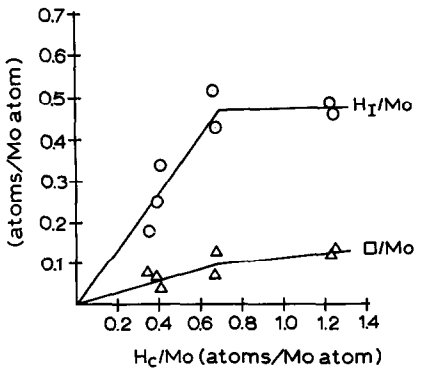

FIG. 2. Irreversibly adsorbed hydrogen (H_I) and anion vacancies formed (□) versus hydrogen consumed (H_C) during reduction of molybdena–alumina.

Infrared Spectroscopy of Adsorbed Pyridine

Figure 4 depicts infrared spectra of pyridine adsorbed on a reduced molybdena–alumina sample (*e*/Mo = 0.39) and desorbed at increasingly higher temperatures, for the spectral region between 1650 and 1450 cm^{-1}. The bands observed in this region, as well as those observed at lower

TABLE 3

Results of Thermogravimetric Analyses

A. Molybdenum on alumina

Desorption temperature	Pyridine uptake (molecules/m^2) × 10^{-18})			
	Oxidized	Reduced 5 min at 670 K	Reduced 1 h at 670 K	Reduced 6 h at 670 K
370 K	1.15	1.24	1.28	1.15
470 K	0.60	0.91	0.73	0.58
570 K	0.25	0.59	0.41	0.34
670 K	0.08	0.40	0.25	0.18

B. Alumina

Desorption temperature	Pyridine uptake (molecules/m^2) × 10^{-18})			
	Oxidized	Reduced 5 min	Reduced 1 h	Reduced 6 h
370 K	1.31	1.16	1.12	1.10
470 K	0.77	0.70	0.66	0.65
570 K	0.60	0.51	0.38	0.38
670 K	0.39	0.32	0.21	0.20

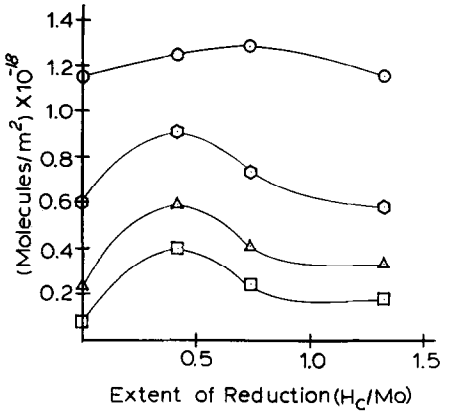

FIG. 3. Pyridine adsorbed on molybdena–alumina following different pretreatments and after evacuations at: (○) 370 K, (○) 470 K, (△) 570 K, and (□) 670 K.

wavenumbers are listed in Table 4. The bands at 1638 and 1540 cm^{-1} can be assigned to pyridine adsorbed on Brønsted acid sites [see Refs. (*23, 24*)]. These two bands disappear after desorption at 570 K. The other bands in the spectra of Fig. 4 are assigned to pyridine adsorbed on Lewis acid sites and they remain even after evacuation at 670 K. In these spectra the contribution from the sample (i.e., the spectrum

TABLE 4

Infrared Absorption Bands of Pyridine in the Region 1700–1000 cm^{-1}

Associated with Brønsted sites (cm^{-1})	Associated with Lewis sites (cm^{-1})
1638	—
—	1621
1614	1616
—	1577
1540	—
1490	1490
—	1450
1246	1242
—	1222
1203	—
1163	—
—	1156
—	1081
—	1071
—	1058

of the sample before exposure to pyridine) has been removed by subtraction. (This subtraction has also been carried out for the spectra shown in Figs. 5 and 6.)

Spectra of pyridine adsorbed on alumina (treated in hydrogen for 5 min) are shown in

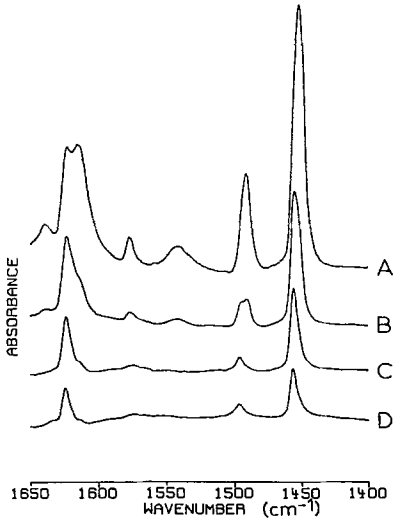

FIG. 4. Infrared spectra of pyridine adsorbed on reduced molybdena–alumina (e/Mo = 0.39) following evacuations at: (A) 370 K, (B) 470 K, (C) 570 K, and (D) 670 K.

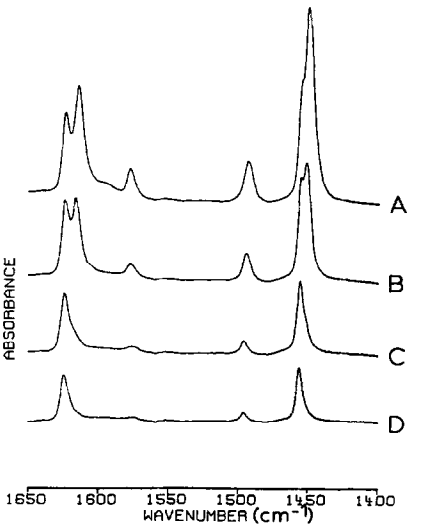

FIG. 5. Infrared spectra of pyridine adsorbed on hydrogen-treated (5 min) alumina following evacuations at: (A) 370 K , (B) 470 K, (C) 570 K, and (D) 670 K.

Fig. 5. Only those peaks corresponding to Lewis acid sites are present. Two peaks are present in the 1450-cm^{-1} region. These are at 1454 and 1450 cm^{-1}. The peak at the lower frequency decreases in intensity and disappears when the sample is evacuated at higher temperatures. The same behavior is observed for the peaks in the 1620-cm^{-1} region (at 1624 and 1615 cm^{-1}). This behavior indicates that two types of Lewis acid sites are present on the alumina surface, one of them being weaker than the other. In fact, the same observation can be made about the peaks in the 1620-cm^{-1} region of the spectra of pyridine on the molybdena–alumina sample (Fig. 4). In the latter case, however, the separation between the peak maxima of the peaks in the 1620-cm^{-1} region is smaller (1621 and 1616 cm^{-1}). The asymmetry of the band near 1450 cm^{-1} for the molybdena–alumina sample also suggests the presence of more than one type of Lewis acid site.

The effect of reduction on the spectra of pyridine adsorbed on molybdena–alumina is displayed in Fig. 6. The spectra were collected after evacuation at 370 K. The peaks corresponding to pyridine adsorbed on Brønsted acid sites are evident only in the spectra of samples oxidized and reduced to low extents, thereby confirming that reduction of the catalyst eliminates Brønsted acidity.

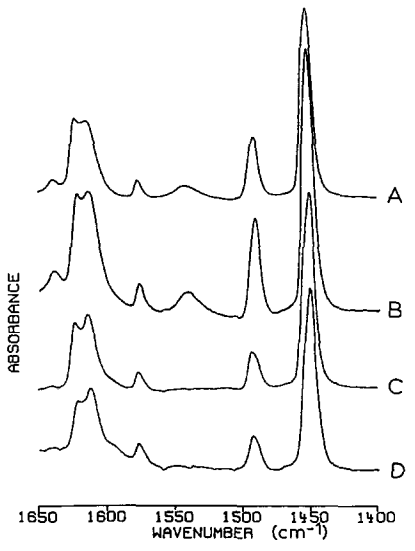

FIG. 6. Infrared spectra of pyridine adsorbed on molybdena–alumina after evacuation at 370 K. (A) Oxidized catalyst, (B) catalyst reduced to e/Mo = 0.39, (C) catalyst reduced to e/Mo = 0.68, (D) catalyst reduced to e/Mo = 1.24.

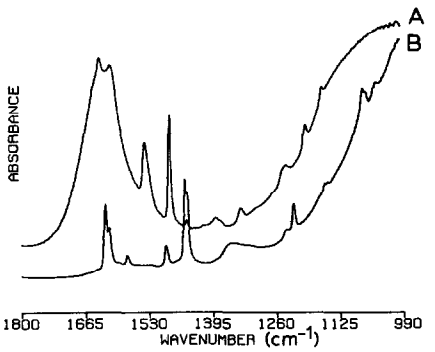

FIG. 7. Infrared spectra of pyridine adsorbed on oxidized alumina, before (B) and after (A) exposure of the sample to HCl.

The integrated areas under the infrared bands at 1450 and 1540 cm^{-1} were used to determine the relative concentrations of the different pyridine species adsorbed on the sample surfaces. For this it was necessary to determine the ratios of the absorptivity coefficients for these absorption peaks. This was done by using a method similar to that described by Kiviat and Petrakis (*13*), as described in detail elsewhere (*18*). In short, it consisted of the conversion of Lewis acid sites into Brønsted acid sites by exposure to 30 Torr of HCl at room temperature. The effect of this treatment on the spectrum of pyridine adsorbed on alumina is shown in Fig. 7. (The infrared spectrum of alumina prior to exposure to pyridine has not been subtracted from the spectra shown in this figure.) Measurements of the spectral area changes accompanying this treatment then allowed the ratio of the absorptivity coefficients (α) for pyridine on Lewis (L) and Brønsted (B) acid sites to be calculated. For each of the two types of Lewis acid sites which were observed, this was done by deconvoluting the band at 1450 cm^{-1} into a low-frequency (LI) and a high-

frequency (LII) component. The results of these measurements are shown in Table 5 for the alumina and molybdena–alumina samples.

Table 6 shows the integrated intensities of the absorption bands at 1450 and 1540 cm^{-1} for pyridine adsorbed on molybdena–alumina and of the band at 1450 cm^{-1} for pyridine adsorbed on alumina. Deconvolution of the band at 1450 cm^{-1}, together with a knowledge of absorptivity coefficient ratios of Table 5, allowed us to calculate ratios of the different types of acid sites. These sites are denoted as pyridine on Brønsted acid sites (BPY) and pyridine on Lewis acid sites corresponding to the low- and high-frequency components of the band at 1450 cm^{-1} (LPY (I) and LPY (II), respectively). The results of these calculations are summarized in Table 7 for the alumina and molybdena–alumina samples.

Combination of Infrared Spectroscopic and Thermogravimetric Results

The results of the infrared spectroscopy studies were combined with the results from the thermogravimetric experiments (Table 3) to obtain estimates of the numbers of each type of acid site on the surface of each sample. The results are listed in Tables 8 and 9. They are expressed in terms of the number of molecules of pyridine adsorbed per square meter of surface. From these tables, trends can be observed for the amounts of pyridine adsorbed on samples reduced to different extents (and compared at the same pyridine evacuation temperature). Figure 8 is a plot of the concentration of Brønsted acid sites versus the extent of reduction (*e*/Mo) of the molybdena–alumina sample. The concentration of Brønsted acid sites increases slightly for low extents of reduction (*e*/Mo = 0.39) but then

TABLE 5

Ratios of Absorptivity Coefficients[a]

Ratio	Alumina	Molybdenum on alumina
$\frac{\alpha^{LI}_{1450}}{\alpha^{B}_{1540}}$	1.80	1.22
$\frac{\alpha^{LII}_{1450}}{\alpha^{B}_{1540}}$	0.925	0.788
$\frac{\alpha^{LI}_{1450}}{\alpha^{LII}_{1450}}$	1.94	1.54

[a] α^{i}_{ν} is the absorptivity coefficient for the peak located near ν (cm^{-1}) that is produced by pyridine adsorbed on i acid sites, where: i = B, Brønsted acid sites; i = LI, weaker Lewis acid sites; and i = LII, stronger Lewis acid sites.

TABLE 6

Integrated Band Intensities for the Bands near 1450 and 1540 cm^{-1}

A. Molybdenum on alumina

Treatment	Pyridine desorption temperature (K)	Area under the 1450-cm^{-1} peak	Area under the 1540-cm^{-1} peak
Oxidized	370	7.28	0.86
	470	3.77	0.13
	570	2.02	0.0
	670	1.16	0.0
Reduced	370	9.88	1.33
e/Mo = 0.39	470	4.58	0.14
	570	2.47	0.08
	670	1.43	0.0
Reduced	370	7.62	0.04
e/Mo = 0.68	470	4.66	0.0
	570	2.60	0.0
	670	1.86	0.0
Reduced	370	6.98	0.0
e/Mo = 1.24	470	4.09	0.0
	570	2.36	0.0
	670	1.44	0.0

B. Alumina

Treatment	Pyridine desorption temperature (K)	Area of the 1450-cm^{-1} peak
Oxidized	370	5.70
	470	3.42
	570	1.83
	670	1.25
Reduced	370	6.90
5 min	470	4.09
	570	2.00
	670	1.34
Reduced 1 h	370	5.44
	470	3.31
	570	1.82
	670	1.23
Reduced 6 h	370	5.00
	470	2.58
	570	1.53
	670	1.05

TABLE 7

Concentration Ratios for Pyridine Adsorbed on the Different Types of Acid Sites on Alumina and Molybdena–Alumina[a]

Pretreatment	Pyridine desorption temperature (K)	Alumina	Molybdena–alumina		
		LPY (I)/LPY (II)	LPY (I)/LPY (II)	LPY (I)/BPY	LPY (Total)/BPY
Oxidized	370	2.09	2.30	5.42	7.77
overnight at	470	1.08	0.917	14.33	30.0
770 K	570	0.238	0.610	—	—
	670	0.147	0.378	—	—
Reduced in H_2	370	2.52	1.62	4.36	7.06
5 min at	470	1.71	0.459	11.6	36.8
670 K	570	0.216	0.294	7.73	34.0
	670	0.166	0.250	—	—
Reduced in H_2	370	4.46	2.38	130.0	184.0
1 h at	470	1.74	1.84	—	—
670 K	570	0.486	1.10	—	—
	670	0.341	0.515	—	—
Reduced in H_2	370	5.42	7.59	—	—
6 h at	470	1.02	2.10	—	—
670 K	570	0.472	0.824	—	—
	670	0.333	0.332	—	—

[a] LPY (I) represents the amount of pyridine adsorbed on the weaker type of Lewis acid site; LPY (II) represents pyridine adsorbed on stronger Lewis acid sites; BPY represents the amount of pyridine adsorbed on Brønsted acid sites.

becomes zero as the catalyst is reduced further. Figure 9 indicates that the concentration of the weaker type of Lewis acid site on molybdena–alumina undergoes an initial increase and then a decrease with extent of reduction. On alumina, the concentration of this site is not altered by treatment in hydrogen. Figure 10 shows that the concentration of the stronger type of Lewis acid site on molybdena–alumina goes through a maximum with extent of reduction at e/Mo = 0.39 and then decreases. On alumina the concentration of this type of site decreases

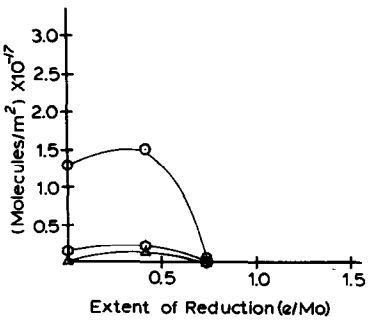

FIG. 8. Amount of pyridine adsorbed on Brønsted acid sites versus extent of reduction of molybdena–alumina, after evacuations at: (○) 370 K, (◯) 470 K, and (△) 570 K.

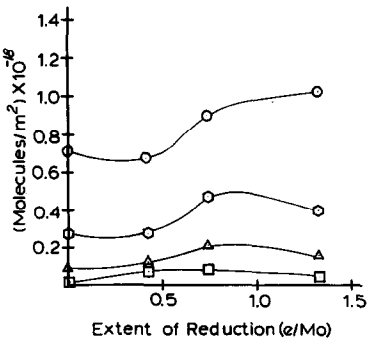

FIG. 9. Amount of pyridine adsorbed on the weaker Lewis acid sites (LPY (I)) versus extent of reduction of molybdena–alumina. (○) after evacuation at 370 K, (◯) after evacuation at 470 K, (△) after evacuation at 570 K, (□) after evacuation at 670 K.

TABLE 8

Amount of Pyridine Adsorbed on Each Type of Lewis Acid Site on Alumina

Pretreatment	Pyridine desorption temperature (K)	(Molecules/m²) × 10^{-18}	
		LPY (I)	LPY (II)
Oxidized overnight at 770 K	370	0.887	0.423
	470	0.400	0.370
	570	0.115	0.485
	670	0.050	0.340
Reduced 5 min at 670 K	370	0.830	0.330
	470	0.442	0.258
	570	0.091	0.419
	670	0.046	0.274
Reduced 1 h at 670 K	370	0.915	0.205
	470	0.419	0.241
	570	0.124	0.256
	670	0.053	0.157
Reduced 6 h at 670 K	370	0.929	0.171
	470	0.328	0.322
	570	0.122	0.258
	670	0.050	0.150

initially and then remains constant with time of treatment in hydrogen.

DISCUSSION

The molybdena on the surface of the oxidized molybdena–alumina sample is present in clusters, as is evident from the presence of bands produced by Mo–O–Mo bond vibrations in the Raman spectrum. Infrared spectra of pyridine adsorbed on the surface of this sample indicated the presence of both Lewis and Brønsted acid sites. Only Lewis acidity is present on the parent alumina surface. Two types of Lewis acid sites were observed on both surfaces. Reduction of the molybdena–alumina catalyst with hydrogen causes the total acidity to increase to a maximum and then to decrease as the catalyst is reduced further. The increase in total acidity is caused by a slight increase in Brønsted acidity and a larger increase in the Lewis acidity. When the catalyst is reduced to higher extents (e/Mo > 0.5) the Brønsted acidity is eliminated and the Lewis acidity decreases.

These changes in the acidity of the molybdena–alumina catalyst can be explained in terms of the model discussed recently by Hall (*25*). In this model one views the surface of the catalyst as populated by small clusters of molybdena. The Brønsted acid sites on the oxidized catalyst may be supposed to be alumina hydroxyl groups located close to these molybdena clusters. Lewis acidity is present on the alumina portion of the surface on the oxidized catalyst and on both the alumina and molybdena portions of the reduced catalyst.

TABLE 9

Amount of Pyridine Adsorbed on Each Type of Acid Site on Molybdena–Alumina

Oxidation state	Pyridine desorption temperature (K)	(Molecules/m²) × 10^{-18}		
		BPY	LPY (I)	LPY (II)
Oxidized	370	0.131	0.710	0.309
	470	0.019	0.278	0.303
	570	—	0.095	0.155
	670	—	0.022	0.058
Reduced e/Mo = 0.39	370	0.154	0.671	0.415
	470	0.024	0.279	0.607
	570	0.017	0.130	0.443
	670	—	0.080	0.320
Reduced e/Mo = 0.68	370	0.007	0.897	0.376
	470	—	0.473	0.257
	570	—	0.215	0.195
	670	—	0.085	0.165
Reduced e/Mo = 1.24	370	—	1.016	0.134
	470	—	0.393	0.187
	570	—	0.154	0.186
	670	—	0.045	0.135

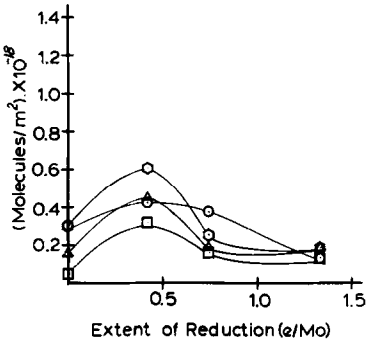

FIG. 10. Amount of pyridine adsorbed on the stronger Lewis acid sites (LPY (II)) versus extent of reduction of molybdena–alumina, after evacuations at (○) 370 K, (○) 470 K, (△) 570 K, and (□) 670 K.

It is now suggested that additional insight can be provided by combining the above model with simple electronegativity concepts. For example, Brønsted acidity is produced on the oxidized molybdena–alumina sample by the presence of the molybdena clusters. Since the average Sanderson electronegativity of Al_2O_3 is 3.72 while that of MoO_3 is 3.89 (*26*), it is possible that hydroxyl groups on alumina which are near molybdena clusters may be made more acidic by inductive effects. (In general, higher electronegativities are associated with stronger acid sites.)

When the catalyst is reduced to low extents (e/Mo $\leq$ 0.39) the Brønsted acidity is observed to increase. Hall and co-workers (*11, 25*) have shown that the bridging oxygen atoms located between molybdenum and aluminum atoms are the first to be attacked during reduction, thereby producing an increase in the number of alumina hydroxyl groups near molybdena clusters. These newly formed hydroxyls would be expected to constitute Brønsted acid sites due to the aforementioned inductive effects of molybdena on alumina. A small number of acidic Mo–OH groups could also form during the initial stages of reduction. The number of Brønsted acid sites formed during this reduction process is much smaller than the amount of hydrogen added to the surface, as can be seen by comparing Figs. 2 and 8. As the molybdena clusters are further reduced, their electronegativity decreases. For example, the average electronegativity of MoO_2 is 3.53, lower than that of Al_2O_3. Therefore, the alumina hydroxyl groups located in close proximity to the molybdena clusters will become less acidic and the Brønsted acidity will disappear during this phase of the reduction process. This decrease in electronegativity is apparently more important than the total amount of hydrogen on the sample, since the latter does not decrease with further extent of reduction (see Fig. 2) while the Brønsted acidity vanishes (see Fig. 8).

The changes in Lewis acidity with reduction of molybdena–alumina can be explained in a similar way. The initial increase in Lewis acidity may be due to generation of anion vacancies on molybdenum (see Fig. 2) and to an increase in the area of the uncovered portions of the alumina surface as the Mo–O–Al bonds are broken during reduction. Evidence for the latter is that the number of Lewis acid sites created upon reduction (e.g., 3×10^{17} m^{-2} for e/Mo = 0.4) is larger than the corresponding number of anion vacancies formed (1×10^{17} m^{-2} for the same extent of reduction (H_C/Mo $\approx$ 0.37), see Fig. 2). As is evident from Figs. 9 and 10, the increase in the number of Lewis acid sites is caused primarily by an increase in number of the strong type of Lewis acid sites. These sites may be covered preferentially by the molybdena polyanions during the genesis of the catalyst. Therefore, when the alumina surface is uncovered upon reduction, some of the stronger Lewis sites will be exposed. Moreover, the strength of the Lewis acid sites near the molybdena clusters will be increased by the increased electronegativity of alumina produced by the presence of molybdena. In addition, some Lewis acid sites can also be associated with the anion vacancies formed on the molybdena clusters as the molybdenum is initially reduced. The latter sites should also be strong Lewis acid sites in view of the high electronegativity of molybdena. When the catalyst is reduced further, the electronegativity of the system decreases, making the Lewis acid sites (both on the alumina and on the molybdena) weaker. This explains the decrease in Lewis acidity observed at the higher extents of reduction. From Figs. 9 and 10 it can be noted that the stronger Lewis acid sites reach a maximum concentration at lower extents of reduction than do the weaker Lewis acid sites. This can be explained by the conversion of stronger Lewis acid sites into weaker sites as the electronegativity of molybdena decreases.

For the alumina surface it was observed that the Lewis acidity decreased when the

catalyst was treated in hydrogen. The stronger type of Lewis acid site is most affected by the hydrogen treatment. This may be caused by hydrogen adsorption on the alumina surface. Amenomiya (*27*) studied the adsorption of hydrogen on γ-alumina. He observed strong adsorption of hydrogen on alumina at high temperatures (720 K). This adsorption occurred mainly at defects on the alumina surface. Thus, the decrease in the number of Lewis acid sites may be caused by adsorption of hydrogen on these sites during the hydrogen treatment.

CONCLUSIONS

Infrared spectroscopy and thermogravimetric analysis of adsorbed pyridine were used to measure the acidity of a molybdena–alumina catalyst and of the alumina used in preparation thereof. Volumetric measurements of hydrogen and oxygen consumed during reduction/oxidation treatments of the catalyst provided information concerning the oxidation state of the molybdenum cations. The oxidation state of any molybdenum present had a significant effect on the properties of the catalyst, especially when compared to the alumina support.

Brønsted acid sites were observed on both oxidized and slightly reduced (e/Mo = 0.39) molybdena–alumina catalysts. Such sites were not present on the alumina support alone. This acidity was eliminated via further reduction of the catalyst. Lewis acid sites were observed on both the alumina and molybdena–alumina catalyst surfaces. Infrared spectra of adsorbed pyridine indicated that these sites were of two types, having different acid strengths.

Based on these results, a model for the molybdena–alumina catalyst was proposed. In terms of this model, the principal role of the molybdena is to alter the electronegativity of alumina in close proximity to molybdena, thereby causing the observed changes in the acid properties.

ACKNOWLEDGMENTS

We would like to thank the Graduate and Professional Opportunities Program (GPOP) for providing a fellowship to one of us (W.S.). We also express our appreciation to Jim Wilson, Bill Kovats, Jerry Vogler, and Nelson Cardona-Martinez for their experimental assistance during various stages of this project.

REFERENCES

1. Schuit, G. C. A., and Gates, B. C., *AIChE J.* **19,** 417 (1973).
2. Massoth, F. E., "Advances in Catalysis," Vol. 27, p. 265. Academic Press, New York, 1978.
3. Grange, P., *Catal. Rev.-Sci. Eng.* **21,** 135 (1980).
4. Jeziorowsky, H., and Knözinger, H., *J. Phys. Chem.* **83,** 1166 (1979).
5. Wang, L., and Hall, W. K., *J. Catal.* **66,** 251 (1980).
6. Cheng, C. P., and Schrader, G. L., *J. Catal.* **60,** 276 (1979).
7. Wang, L., and Hall, W. K., *J. Catal.* **77,** 232 (1982).
8. Massoth, F. E., *J. Catal.* **30,** 204 (1973).
9. Hall, W. K., and Massoth, F. E., *J. Catal.* **34,** 41 (1974).
10. Hall, W. K., and Lo Jacono, M., *in* "Proceedings, 6th International Congress on Catalysis, London, 1976" (G. C. Bond, P. B. Wells, and F. C. Tompkins, Eds.), Vol. 1, p. 246. The Chemical Society, London, 1977.
11. Millman, W. S., Crespin, M., Cirillo, A. C., Abdo, S., and Hall, W. K., *J. Catal.* **60,** 404 (1979).
12. Parry, E. P., *J. Catal.* **2,** 371 (1963).
13. Kiviat, F. E., and Petrakis, L., *J. Phys. Chem.* **77,** 1232 (1973).
14. Mone, R., and Moscow, L., *Prepr. Amer. Chem. Soc., Div. Pet. Chem.* **20,** 564 (1975).
15. Mone, R., *in* "Preparation of Catalysts" (J. A. Delmon, P. A. Jacobs, and G. Poncelet, Eds.). Elsevier, New York, 1976.
16. Segawa, K., and Hall, W. K., *J. Catal.* **76,** 133 (1982).
17. Segawa, K., and Hall, W. K., *J. Catal.* **77,** 221 (1982).
18. Suarez, W., M.S. thesis. Department of Chemical Engineering, University of Wisconsin, 1984.
19. Wilson, J. H., M.S. thesis. Department of Chemical Engineering, University of Wisconsin, 1980.
20. Kovats, W. D., Ph.D. thesis. Department of Chemical Engineering, University of Wisconsin, 1984.
21. Wang, L., and Hall, W. K., *J. Catal.* **83,** 242 (1983).
22. Cirillo, A. C., Dollish, F. R., and Hall, W. K., *J. Catal.* **62,** 379 (1980).

23. Little, L. H., "Infrared Spectra of Adsorbed Species." Academic Press, New York, 1966.
24. Tanabe, K., *in* "Catalysis, Science and Technology" (J. R. Anderson and M. Boudart, Eds.), Vol. 2. Springer-Verlag, New York, 1981.
25. Hall, W. K., "Proceedings, 4th International Conference: The Chemistry and Uses of Molybdenum." Golden, Colorado, 1982.
26. Sanderson, R. T., "Inorganic Chemistry." Reinhold, New York, 1967.
27. Amenomiya, J., *J. Catal.* **22,** 109 (1971).